NASA TECHNICAL NOTE

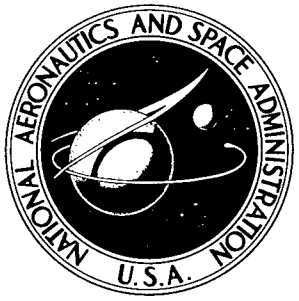


NASA TN D-3111

NASA TN D-3111



# BUCKLING AND POSTBUCKLING TESTS OF RING-STIFFENED CIRCULAR CYLINDERS LOADED BY UNIFORM EXTERNAL PRESSURE

*by Donaldson A. Dow*

*Langley Research Center*
*Langley Station, Hampton, Va.*



NATIONAL AERONAUTICS AND SPACE ADMINISTRATION • WASHINGTON, D. C. • NOVEMBER 1965

NASA TN D-3111

# BUCKLING AND POSTBUCKLING TESTS OF RING-STIFFENED CIRCULAR CYLINDERS LOADED BY UNIFORM EXTERNAL PRESSURE

By Donaldson A. Dow

Langley Research Center
Langley Station, Hampton, Va.

NATIONAL AERONAUTICS AND SPACE ADMINISTRATION

For sale by the Clearinghouse for Federal Scientific and Technical Information
Springfield, Virginia 22151 – Price $1.00

# BUCKLING AND POSTBUCKLING TESTS OF RING-STIFFENED CIRCULAR CYLINDERS LOADED BY UNIFORM EXTERNAL PRESSURE

By Donaldson A. Dow
Langley Research Center

## SUMMARY

Experimental results are presented for tests of 10 ring-stiffened cylinders loaded to failure by uniform external air pressure. The proportions of the aluminum-alloy cylinders were such that local buckling (instability between rings) occurred before general instability (instability of the rings and skin as a composite wall). Failure by general instability occurred between about 3/4 atmosphere (76 kN/m$^2$) for the weakest cylinder to 3 atmospheres (304 kN/m$^2$) for the strongest.

Test results for local buckling are compared with results from previous tests and with theoretical results. The test cylinders buckled locally at somewhat higher pressures than those of a previous test program but at lower pressures than predicted by classical theory. The result of changes in cylinder geometry on structural efficiency (high-strength, low-mass characteristics) was assessed for the collapse strengths of the cylinders. The study indicated that efficient cylinders have thin skins with many closely spaced low-mass stiffening rings.

## INTRODUCTION

The ring-stiffened cylinder is well suited for supporting external pressure loads and is used extensively for this purpose in submarine hulls. However, little information is available on cylinders designed to carry the low values of pressure of interest in aerospace applications - for example, external pressures on a spacecraft in an abort situation. The present report presents the results of an experimental study of the effect of changes in cylinder geometry on the buckling and failing strength of cylinders which fail at uniformly distributed external differential pressures of between 3/4 and 3 atmospheres (76 kN/m$^2$ and 304 kN/m$^2$). A series of 10 cylinders was tested in which the dimensions of the cylinders were systematically varied. Data are provided on the local buckling and general instability loads for cylinders of geometries where very few test results have been available.

## SYMBOLS

The units used for the physical quantities defined in this paper are given both in U.S. Customary units and in the International System of Units (SI). (See ref. 1.) The appendix presents factors relating these two systems of units.

$b_s$ ring spacing, inches (centimeters)

$C_p$ hydrostatic-pressure buckling coefficient, $\frac{p_{cr} r b_s^2}{D\pi^2}$

$D$ plate flexural stiffness per unit length, $\frac{Et_s^3}{12(1 - \mu^2)}$

$E$ Young's modulus, pounds per square inch (kilonewtons per square meter)

$L$ length of cylinder, inches (centimeters)

$n_{cr}, n_{th}$ number of circumferential full waves at buckling, experimental and theoretical, respectively

$p$ pressure, pounds per square inch (kilonewtons per square meter)

$p_{cr}$ pressure at local buckling, pounds per square inch (kilonewtons per square meter)

$p_f$ collapse pressure, pounds per square inch (kilonewtons per square meter)

$r$ radius of cylinder to skin midplane, inches (centimeters)

$t_s$ thickness of cylinder skin, inches (centimeters)

$t_w$ thickness of ring material, inches (centimeters)

$\bar{t}$ longitudinal cross-sectional area of composite shell per unit length expressed as an equivalent thickness, inches (centimeters)

$Z$ cylinder bay curvature parameter, $\frac{b_s^2}{rt_s}\sqrt{1 - \mu^2}$

$\epsilon$ strain

$\mu$ Poisson's ratio

## TEST SPECIMENS

Dimensions of the test cylinders are given in figure 1 and table I. Figure 1 gives the dimensions that were held constant, and table I lists the dimensions that were varied. The thicknesses given in table I are averages of several micrometer readings.

The cylinders were constructed of bare 2024-T3 aluminum alloy with a compressive yield stress of about 42 ksi (290 $MN/m^2$) and with a proportional limit of about 29 ksi (200 $MN/m^2$). The cylinder skin was fabricated from an aluminum sheet with a single lap joint in the axial direction. The joint was bonded with a sealing compound to make it airtight and then riveted. The Z-section rings were fabricated by spin-forming flat disks onto a machined mandrel; they were later attached to the cylinder wall by spotwelding. The ends of the cylinders were closed by thick aluminum bulkheads. (See fig. 1.)

## TEST APPARATUS

The test apparatus includes equipment for applying pressure to the cylinders and for measuring and recording strains, deflections, and pressures. For the purposes of applying pressure, the test cylinders were placed in a large heavy steel tank (fig. 2). The tank was then sealed, bolted, and connected to an air pressure supply line. During the test, the air pressure in the tank was slowly increased; thus a uniform pressure was exerted on the cylinder wall and ends. Atmospheric pressure was maintained inside the test cylinder throughout the test by means of a vent tube. In the case of cylinder 7, however, the differential pressure needed to fail the cylinder was obtained by connecting the vent tube of this specimen to an air ejector, which lowered the pressure inside the test cylinder to about 4 psia (27.6 $kN/m^2$).

The steel tank had a large plexiglass window. The window provided a means to visually observe and photograph the formation of the buckles, the changes in the buckle pattern, and collapse of the cylinder.

Before a cylinder was placed in the tank, it was instrumented with wire resistance strain gages. (See fig. 3.) The gages helped indicate the pressures at which local buckling and general instability occurred. They also provided load-strain curves which helped to show the behavior of the cylinder in both the prebuckled and the buckled state. In addition to the strain gages, several of the cylinders had instrumentation which measured the axial shortening of the cylinder between the two end rings.

The differential pressure applied to the cylinders was measured throughout the loading period by means of an electrical differential pressure transducing cell mounted on the test cylinder bulkhead. The data from the instrumentation were recorded on the Langley central digital data recording system.

## TEST RESULTS AND DISCUSSION

### Local Buckling

Local buckling was characterized by buckling of the skin between stiffening rings. Buckling normally occurred suddenly with an audible noise. Table II gives the local buckling pressure $p_{cr}$ obtained from load-strain curves for each cylinder. (See fig. 4 for a typical example.) Results are plotted in figure 5(a) on a nondimensional buckling chart. In addition, the data from references 2 and 3 and a theoretical curve from reference 4 are shown for comparison.

The data of the present tests fall in the "transition range" ($10 < Z < 100$). In this range, both the present data and the data of reference 3 are generally well below the theoretical solution; the present results averaging approximately 12 percent low and the results of reference 3 averaging approximately 27 percent low. The test results from reference 3 were for steel cylinders and may be influenced by plasticity. The stress levels at buckling in these cylinders were considerably higher with respect to the yield stress than those of the present tests. It is quite unlikely that plasticity influenced the present test results; cylinder 7 had the highest average prebuckling circumferential stresses which were approximately 9.75 ksi (67.2 $MN/m^2$), well below the proportional limit of 29 ksi (200 $MN/m^2$) for the cylinder material.

The low buckling loads may be the result of the axial stress component of the applied pressure which is shown in reference 4 to have a larger influence on buckling at small values of Z than at large values of Z. Buckling loads of cylinders in pure axial compression are often well below the values given by classical theory. The discrepancy for cylinders in pure axial compression is normally taken to be a function of $r/t_s$. (See, for example, ref. 5.) The discrepancy increases as $r/t_s$ increases. A study of the present test data in figure 5(b) suggests that a similar effect of $r/t_s$ exists for external pressure loading. The data of reference 3 (shown in fig. 5(a)), however, did not show any consistent $r/t_s$ effect; perhaps due to plasticity effects.

The data of references 2 and 3 are in close agreement with the theoretical curve for Z greater than 100 (fig. 5(a)). In this range, the axial component of the applied pressure is less influential than at lower values of Z. In addition, the results are not believed to be affected by plasticity.

The buckling load for a cylinder with a given wall geometry and ring spacing was increased by increasing the thickness of the reinforcing rings. Compare, for example, the results for cylinder 9 with those for cylinder 2, and the results for cylinder 10 with those for cylinder 5, as given in figure 5(b). The heavier rings provide more radial and rotational restraint to the cylinder than the lighter rings and carry a greater portion of the pressure load. These factors presumably account for the increase in buckling pressure.

The number of full waves $n_{cr}$ into which each cylinder buckled, is given in table II. Also given is the theoretical number of waves $n_{th}$ from reference 4. The cylinders always buckled into less waves than predicted, but the difference between test and prediction is generally small. The number of waves $n_{cr}$ was determined by measuring the wavelength from the photographs of the buckled cylinders. (See fig. 6.) Figure 6(a) is a photograph of cylinder 10 in the unbuckled state. Note that the two lines of light are straight and vertical. The appearance of the buckles can be seen in figure 6(b), where the line of light to the right of the cylinder center is curved. The buckles in this cylinder formed on one side of the cylinder before the other side; the rest of the cylinders experienced buckling all around simultaneously. From photographs such as these, the wavelength and the number of waves can be approximated.

## General Instability

All the cylinders tested in this program had collapse pressures substantially greater than local buckling pressures; thus, after local buckling, the cylinders still had a load-carrying capability. As the pressure load increased, the buckling deformations increased (fig. 6(c)). Many of the cylinders experienced a change in the number of buckles; some experienced more than one change. The number of buckles always appeared to decrease rather than increase. This change was both heard and seen, and the new buckle pattern was then photographed. By comparing the photographs of figures 6(c) and 6(d), for instance, the change in the buckle pattern of cylinder 10 can be noted. Just prior to the collapse of the cylinders, the buckles were extremely deep as can be seen from figure 6(e).

In the unbuckled state, the axial shortening of the cylinders was very small. At buckling, however, the shortening immediately increased to about 10 times the prebuckled value and then increased nearly linearly with applied pressure until shortly before collapse; at this time there was an increase in the rate of shortening with applied pressure. Figure 7 shows a typical pressure—axial-shortening curve. The total shortening just prior to collapse was quite large, often about 1 percent of the length of the cylinder. Buckling deformations were also large.

The cylinders continued to take additional pressure until general instability load or collapse load was reached. At this time the rings and skin failed as a composite shell. Figure 6(f) shows cylinder 10 shortly after collapse. The failing pressure $p_f$ and the ratio of the failing pressure to the local buckling pressure $p_f/p_{cr}$ for each cylinder is shown in table II.

The collapse pressures are plotted on a structural efficiency plot in figure 8. The mass index $\bar{t}/r$ of each cylinder is plotted against the structural index $p_f/E$. A comparison of different $r/t_s$ curves indicates that thin skins with many rings are more efficient than thick skins with few rings. In addition, note that the test points for cylinders 9 and 10 $\left(t_w/t_s = 0.8\right)$ are slightly above the curves for cylinders with the lighter rings $\left(t_w/t_s = 0.5\right)$. Thus, it

appears that cylinder efficiency may also be improved by using rings of a thinner material. Hence, it would appear that the most efficient cylinders would have thin skins with many closely spaced low-mass stiffening rings.

## CONCLUDING REMARKS

The results of tests on 10 ring-stiffened cylinders, loaded to failure by external pressure, have been presented and discussed. The test cylinders were designed such that local buckling would occur at pressures lower than collapse pressures. A comparison of local buckling pressures, with other test data and with theory, showed that the test cylinders buckled at pressures higher than those of a previous test program but lower than the results predicted by classical theory. The tests also showed that a highly buckled cylinder loaded by external pressure could carry a pressure substantially above the local buckling pressure. A study of the structural efficiency of the cylinders indicates that efficient cylinders have thin skins with many closely spaced low-mass stiffening rings.

Langley Research Center,
National Aeronautics and Space Administration,
Langley Station, Hampton, Va., September 3, 1965.

## APPENDIX

## CONVERSION OF U.S.CUSTOMARY UNITS TO SI UNITS

The International System of Units (SI) was adopted by the Eleventh General Conference on Weights and Measures, Paris, October 1960, in Resolution No. 12 (ref. 1). Conversion factors for the units used herein are given in the following table:

| Physical Quantity | U.S. Customary Unit | Conversion factor (*) | SI unit |
|---|---|---|---|
| Length . . . . . | in. | 0.0254 | meters (m) |
| Stress . . . . . | ksi = kips/in$^2$ | 6.895 × 10$^6$ | newtons per square meter (N/m$^2$) |
| Pressure . . . . | psi = lbf/in$^2$ | 6.895 × 10$^3$ | newtons per square meter (N/m$^2$) |

*Multiply value given in U.S. Customary Unit by conversion factor to obtain equivalent value in SI unit.

Prefixes to indicate multiple of units are as follows:

| Prefix | Multiple |
|---|---|
| mega (M) | 10$^6$ |
| kilo (k) | 10$^3$ |
| centi (c) | 10$^{-2}$ |

## REFERENCES


1. Mechtly, E. A.: The International System of Units - Physical Constants and Conversion Factors. NASA SP-7012, 1964.

2. Sturm, Rolland George: A Study of the Collapsing Pressure of Thin-Walled Cylinders. Bull. No. 329, Eng. Expt. Sta., Univ. Illinois, 1941.

3. Widenburg, Dwight F.; and Trilling, Charles: Collapse by Instability of Thin Cylindrical Shells Under External Pressure. Trans. ASME, vol. 56, no. 11, Nov. 1934, pp. 819-825.

4. Batdorf, S. B.: A Simplified Method of Elastic-Stability Analysis for Thin Cylindrical Shells. NACA Rept. 874, 1947. (Formerly included in NACA TN's 1341 and 1342.)

5. Gerard, George; and Becker, Herbert: Handbook of Structural Stability. Part III - Buckling of Curved Plates and Shells. NACA TN 3783, 1957.

TABLE I.- DIMENSIONS OF TEST CYLINDERS

| Cylinder | Ring spacing, $b_s$ | | Skin thickness, $t_s$ | | Ring thickness, $t_w$ | | $r/t_s$ | $b_s/t_s$ | $t_w/t_s$ | $\bar{t}/t_s$ |
|---|---|---|---|---|---|---|---|---|---|---|
| | in. | cm | in. | cm | in. | cm | | | | |
| 1 | 2.50 | 6.35 | 0.0332 | 0.0843 | 0.0151 | 0.0384 | 421 | 75.3 | 0.455 | 1.258 |
| 2 | 3.75 | 9.53 | .0332 | .0843 | .0152 | .0386 | 421 | 113.0 | .458 | 1.173 |
| 3 | 5.00 | 12.70 | .0335 | .0851 | .0148 | .0376 | 418 | 149.3 | .442 | 1.126 |
| 4 | 2.50 | 6.35 | .0405 | .1029 | .0212 | .0538 | 346 | 61.7 | .524 | 1.294 |
| 5 | 3.75 | 9.53 | .0402 | .1021 | .0208 | .0528 | 348 | 93.3 | .517 | 1.195 |
| 6 | 5.00 | 12.70 | .0404 | .1026 | .0203 | .0516 | 347 | 123.8 | .503 | 1.142 |
| 7 | 3.75 | 9.53 | .0534 | .1356 | .0258 | .0655 | 262 | 70.2 | .483 | 1.180 |
| 8 | 5.00 | 12.70 | .0530 | .1346 | .0249 | .0632 | 264 | 94.3 | .470 | 1.132 |
| 9 | 3.75 | 9.53 | .0334 | .0848 | .0263 | .0668 | 419 | 112.3 | .787 | 1.293 |
| 10 | 3.75 | 9.53 | .0407 | .1034 | .0332 | .0843 | 344 | 92.1 | .816 | 1.301 |

TABLE II.- TEST RESULTS

| Cylinder | Pressure at local buckling, $p_{cr}$ | | Collapse pressure, $p_f$ | | $p_f/p_{cr}$ | $n_{cr}$ | $n_{th}$ |
|---|---|---|---|---|---|---|---|
| | psi | $kN/m^2$ | psi | $kN/m^2$ | | | |
| 1 | 13.8 | 95.1 | 21.5 | 148 | 1.56 | 20 | 25 |
| 2 | 8.66 | 59.7 | 14.3 | 99 | 1.65 | 16 | 21 |
| 3 | 7.17 | 49.4 | 12.9 | 89 | 1.80 | 16 | 19 |
| 4 | 27.0 | 186 | 32.8 | 226 | 1.21 | 20 | 23 |
| 5 | 15.9 | 110 | 21.8 | 150 | 1.37 | 18 | 20 |
| 6 | 12.4 | 85.5 | 18.5 | 128 | 1.49 | 17 | 18 |
| 7 | 37.2 | 256 | 45.9 | 316 | 1.23 | 17 | 19 |
| 8 | 24.5 | 169 | 28.6 | 197 | 1.17 | 12 | 17 |
| 9 | 9.62 | 66.3 | 20.0 | 138 | 2.08 | 21 | 21 |
| 10 | 17.5 | 121 | 29.8 | 205 | 1.70 | 19 | 20 |

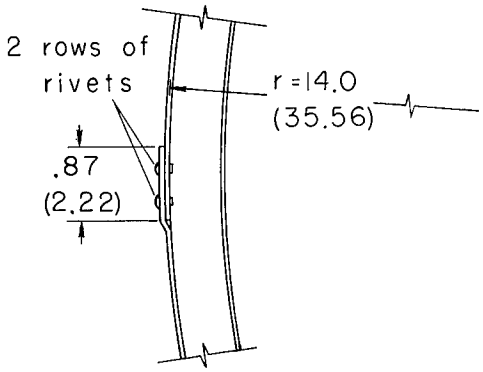


Splice detail

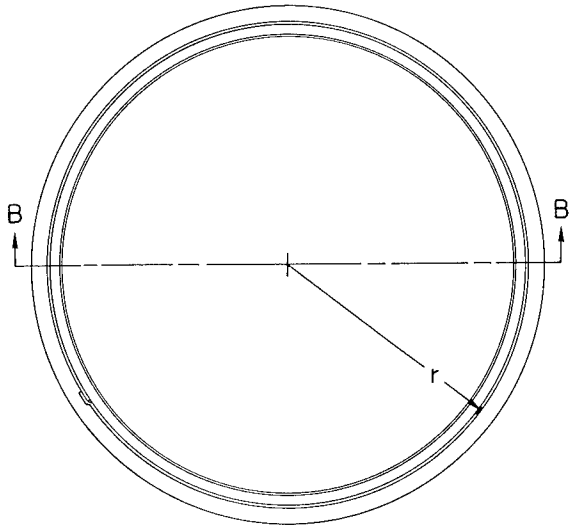


Section A-A

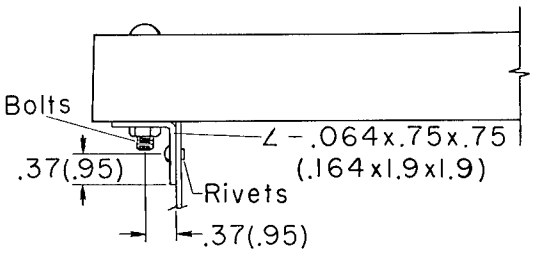


End ring detail

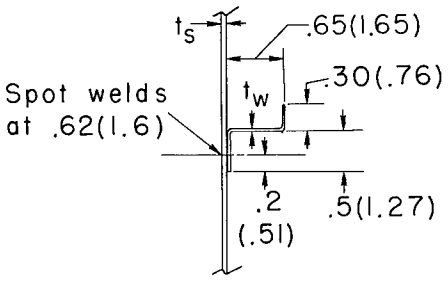


Stiffening ring detail

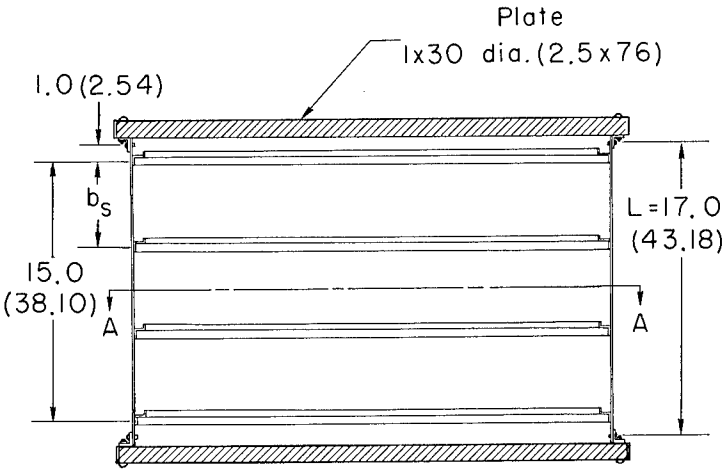


Section B-B

Figure 1.- Dimensions of cylinders. All dimensions are in inches (centimeters). (See table I.)

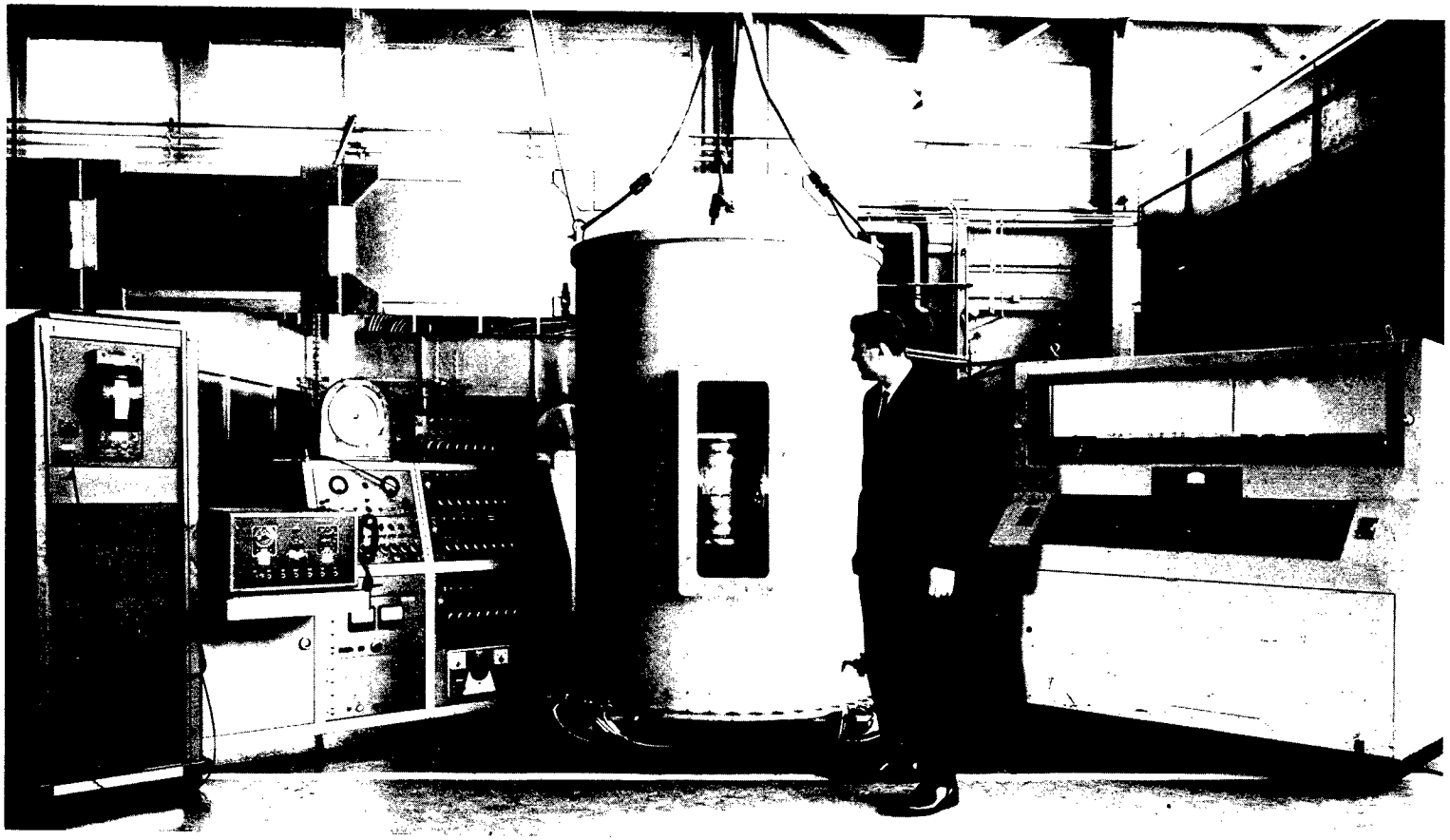

Figure 2.- General view of test setup showing a cylinder in the pressurizing tank. L-64-3159

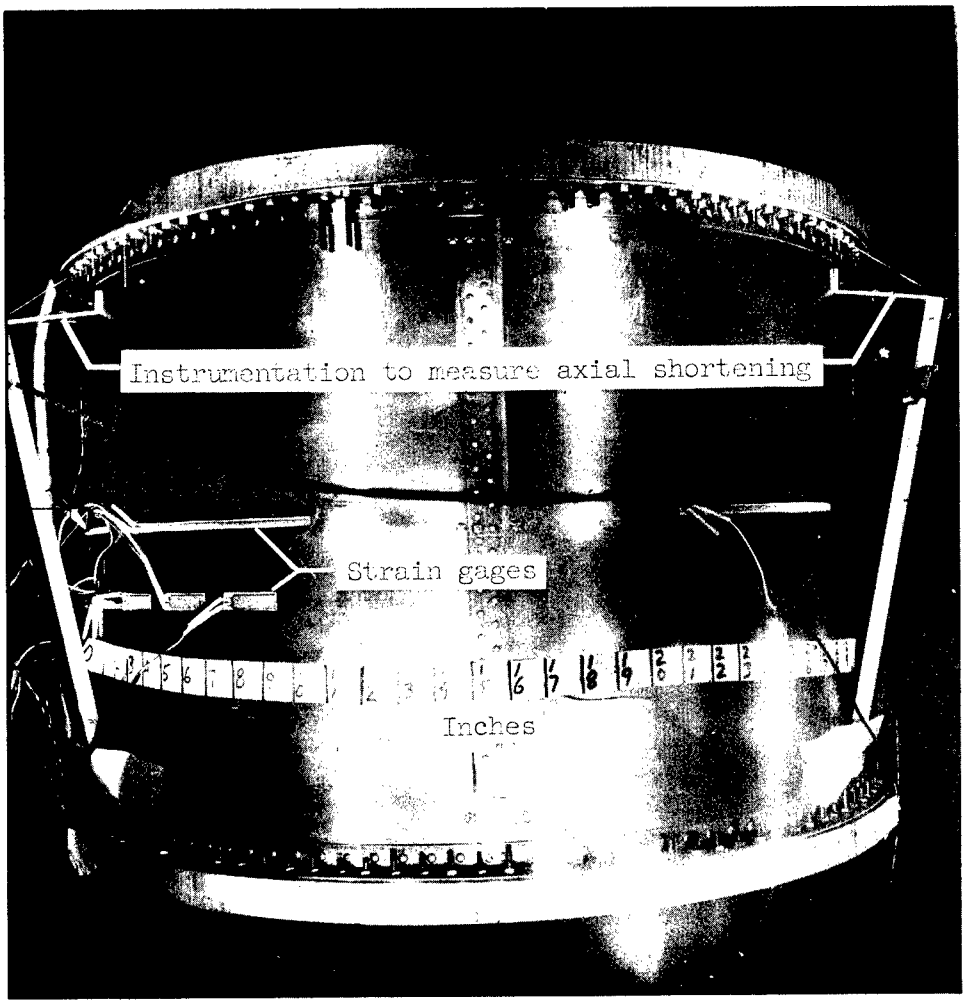


L-65-7903

Figure 3.- View of fully instrumented cylinder (number 9) through window of pressurizing tank.

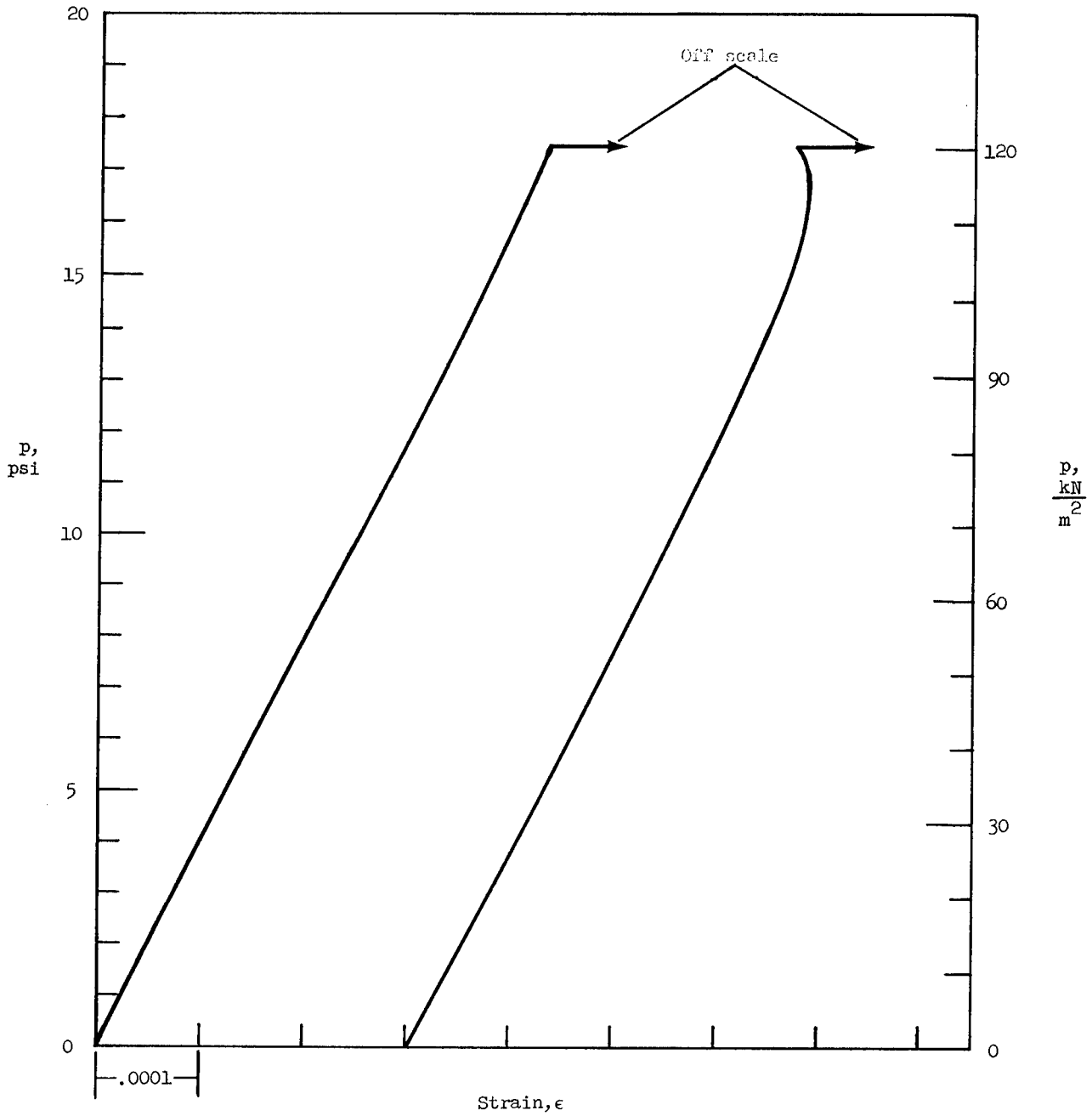


Figure 4.- Load-strain curve showing local buckling pressure of cylinder 10.

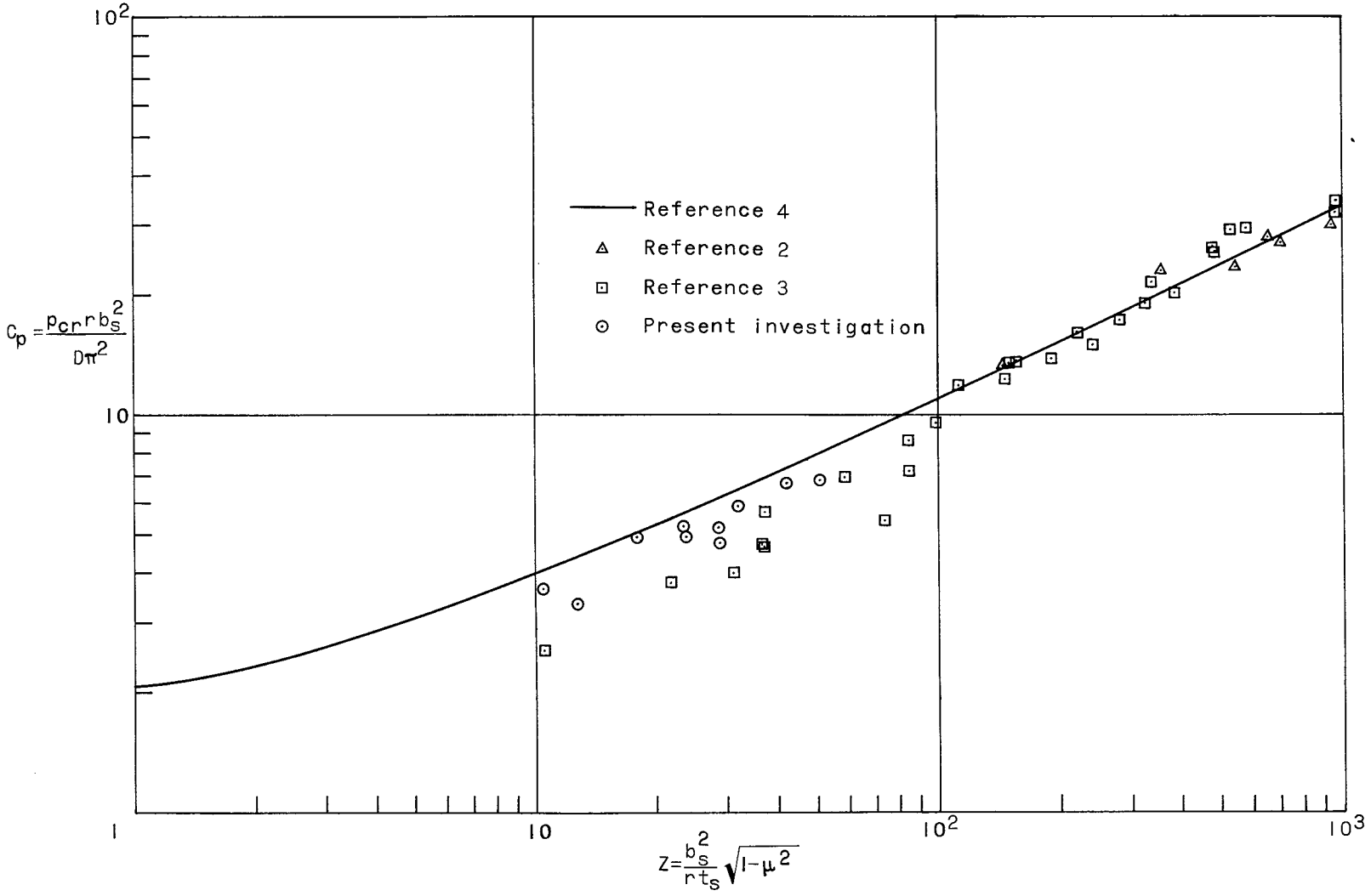


(a) $1 \leq Z \leq 10^3$; test data from present investigation and references 2 and 3.

Figure 5.- Comparison of experimental and theoretical results for local buckling under external pressure.

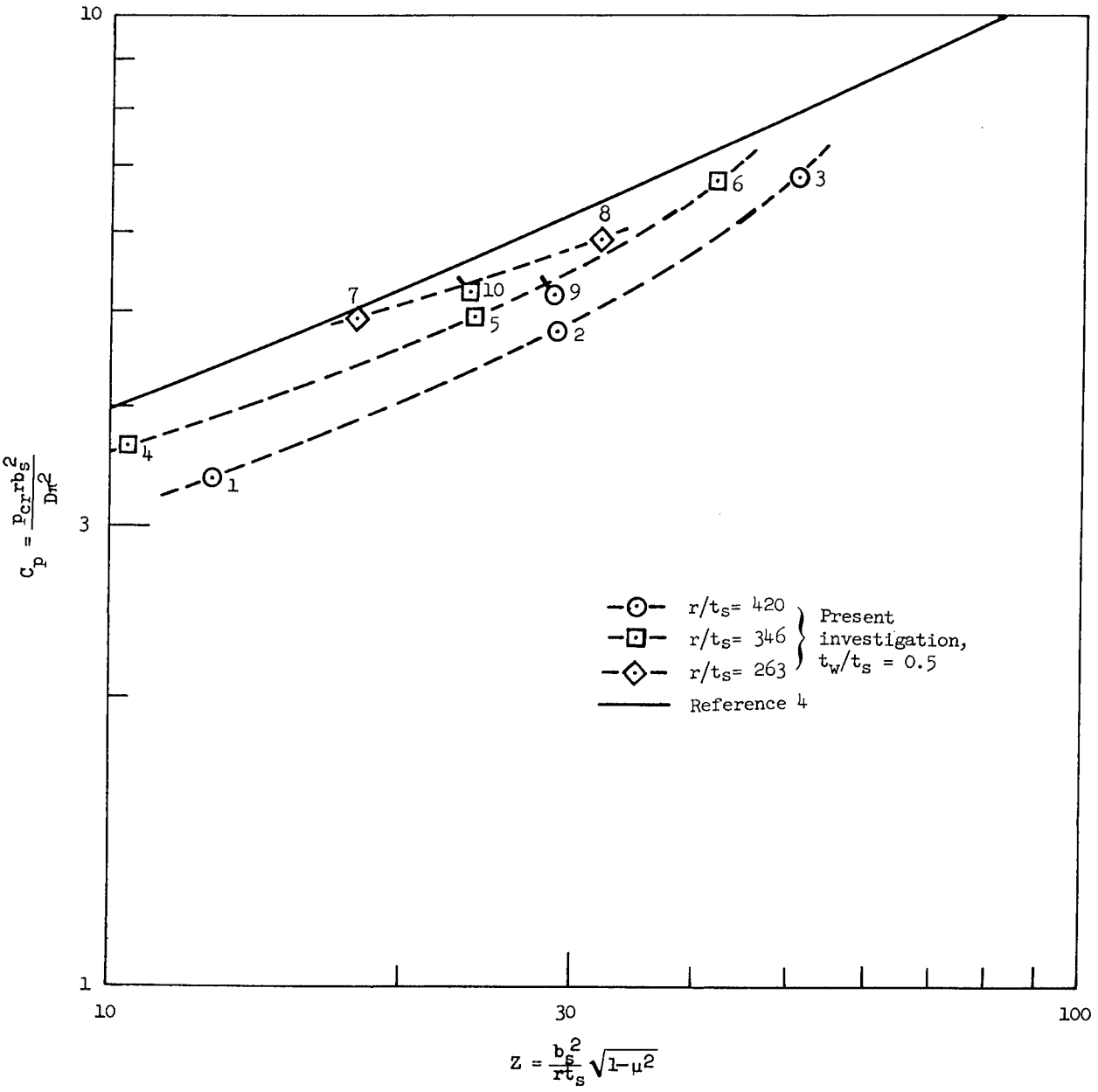


(b) $10 \leqq Z \leqq 100$; present data showing the effect of $r/t_s$ on the buckling coefficient; numbers beside test points denote cylinder number; symbols with ticks indicate $t_w/t_s = 0.8$.

Figure 5.- Concluded.

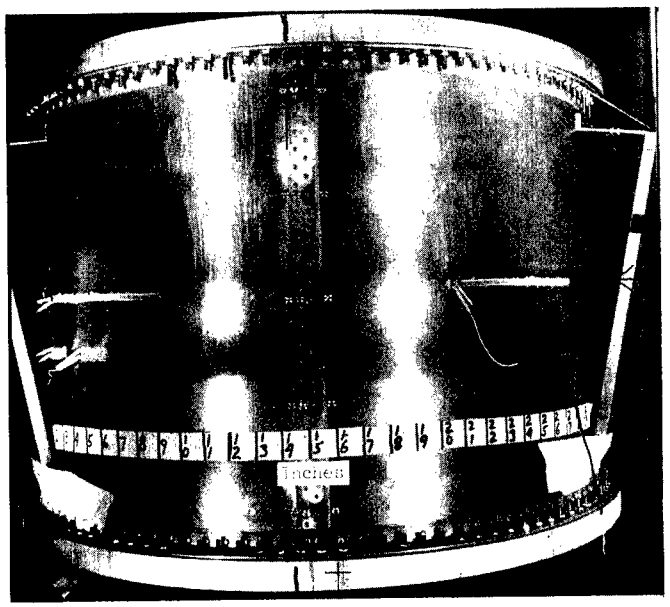

(a) Cylinder in unbuckled state. (Note straight lines of light.) Pressure, 0 psi $\left(0\ kN/m^2\right)$.

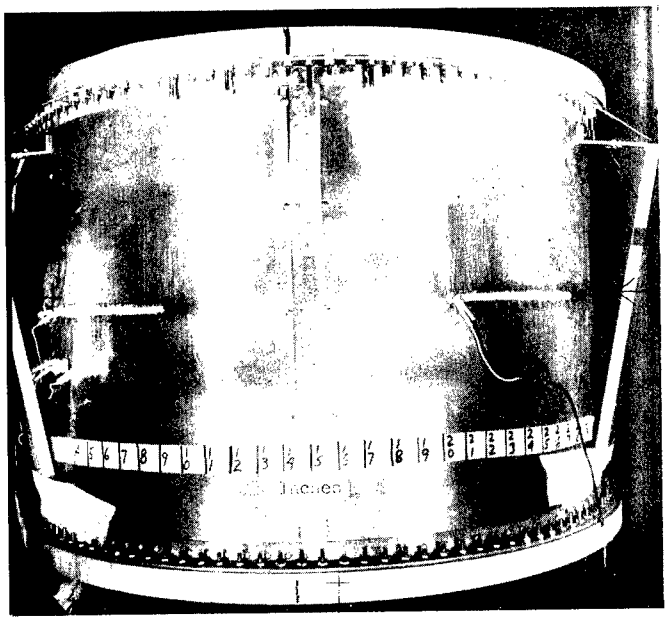

(b) Cylinder immediately after first buckling. (Note one line of light is curved.) Pressure, 17.6 psi $\left(121\ kN/m^2\right)$.

L-65-7904

Figure 6.- Photographs of cylinder 10 at various stages of buckling.

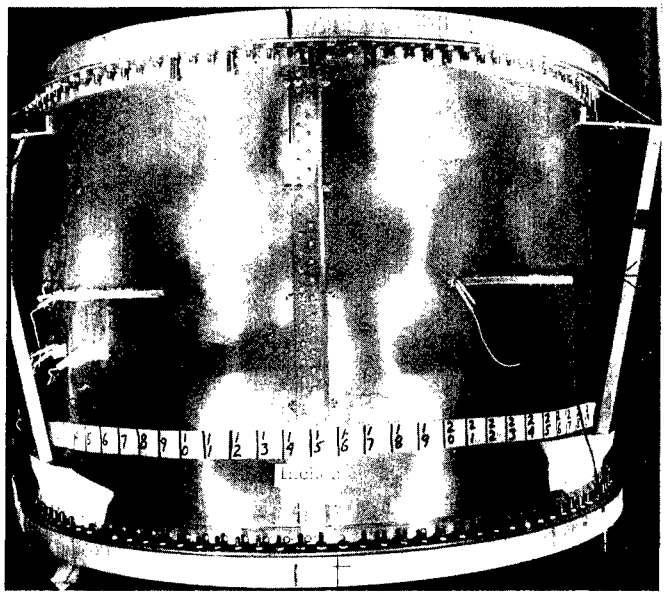

(c) Cylinder with buckles all around. Pressure, 19.0 psi $\left(131\ kN/m^2\right)$.

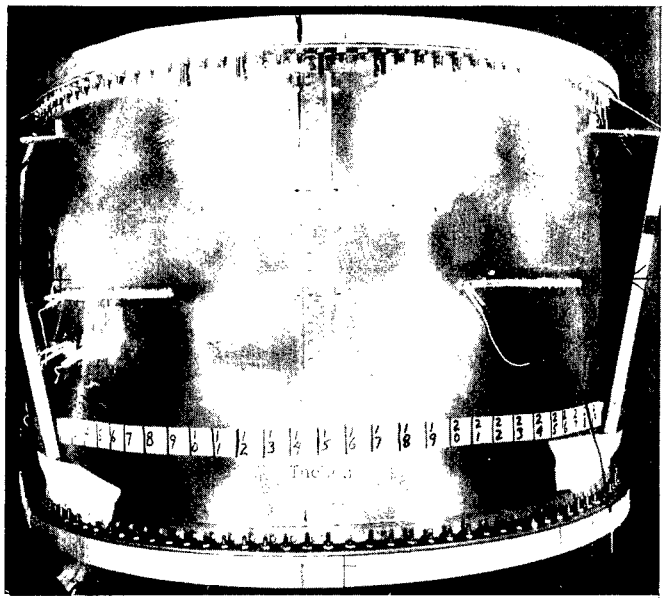

(d) Change in buckle pattern. (Compare with fig. 5(c).) Pressure, 22.3 psi $\left(154\ kN/m^2\right)$.

Figure 6.- Continued. L-65-7905

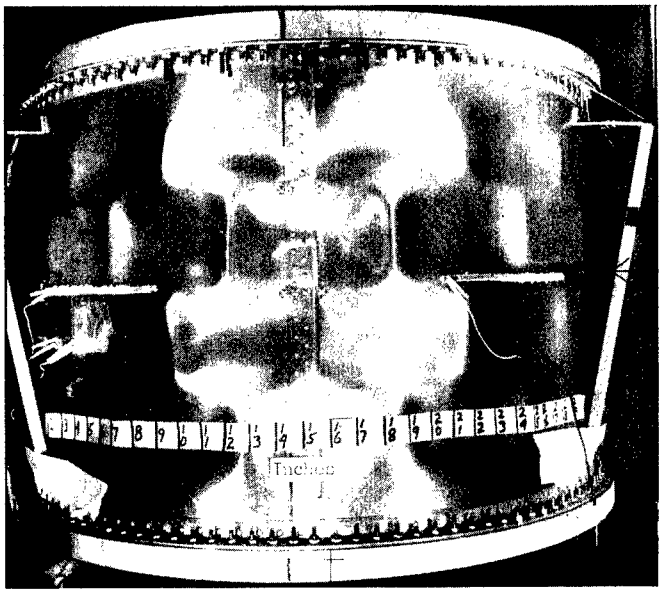

(e) Cylinder with very deep buckles. Pressure, 29.6 psi $\left(204\ kN/m^2\right)$.

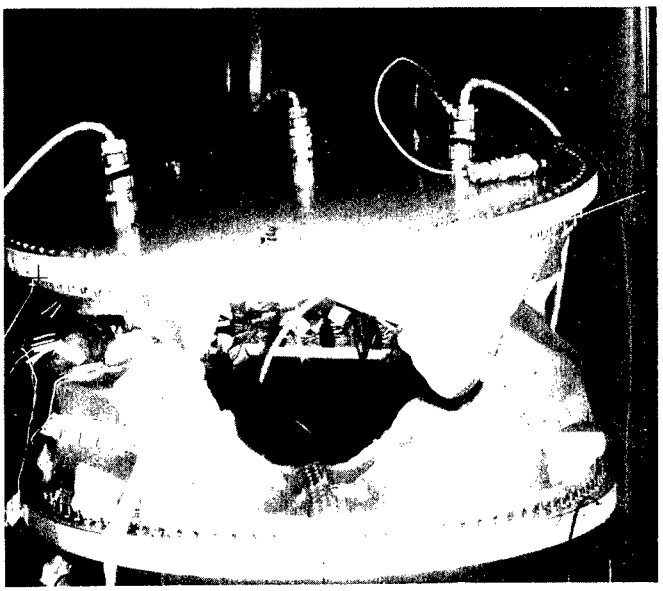

(f) Collapse. Pressure immediately before collapse, 29.8 psi $\left(206\ kN/m^2\right)$.

Figure 6.- Concluded. L-65-7906

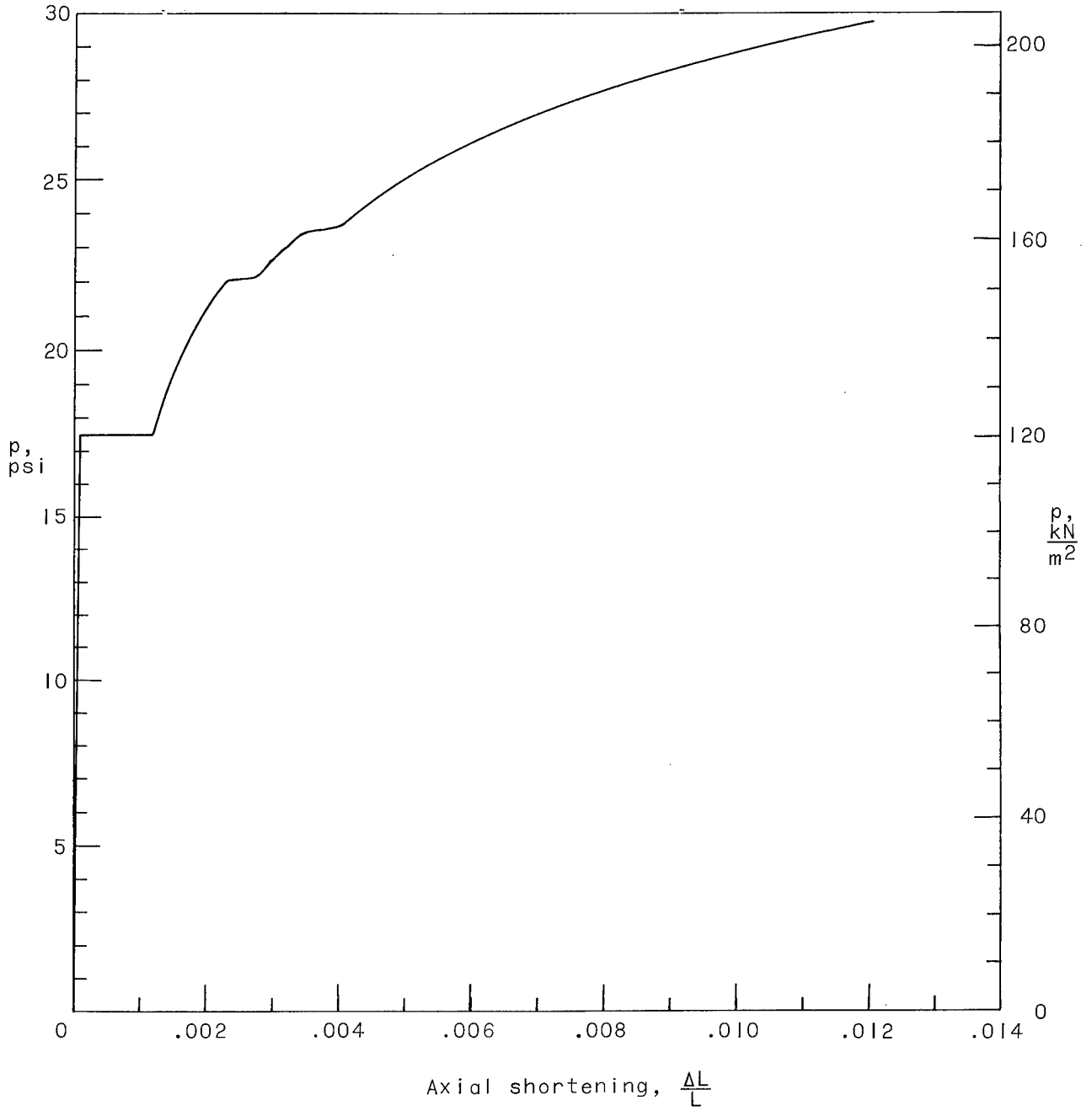


Figure 7.- Curve showing axial shortening with pressure for one of the axial shortening devices on cylinder 10.

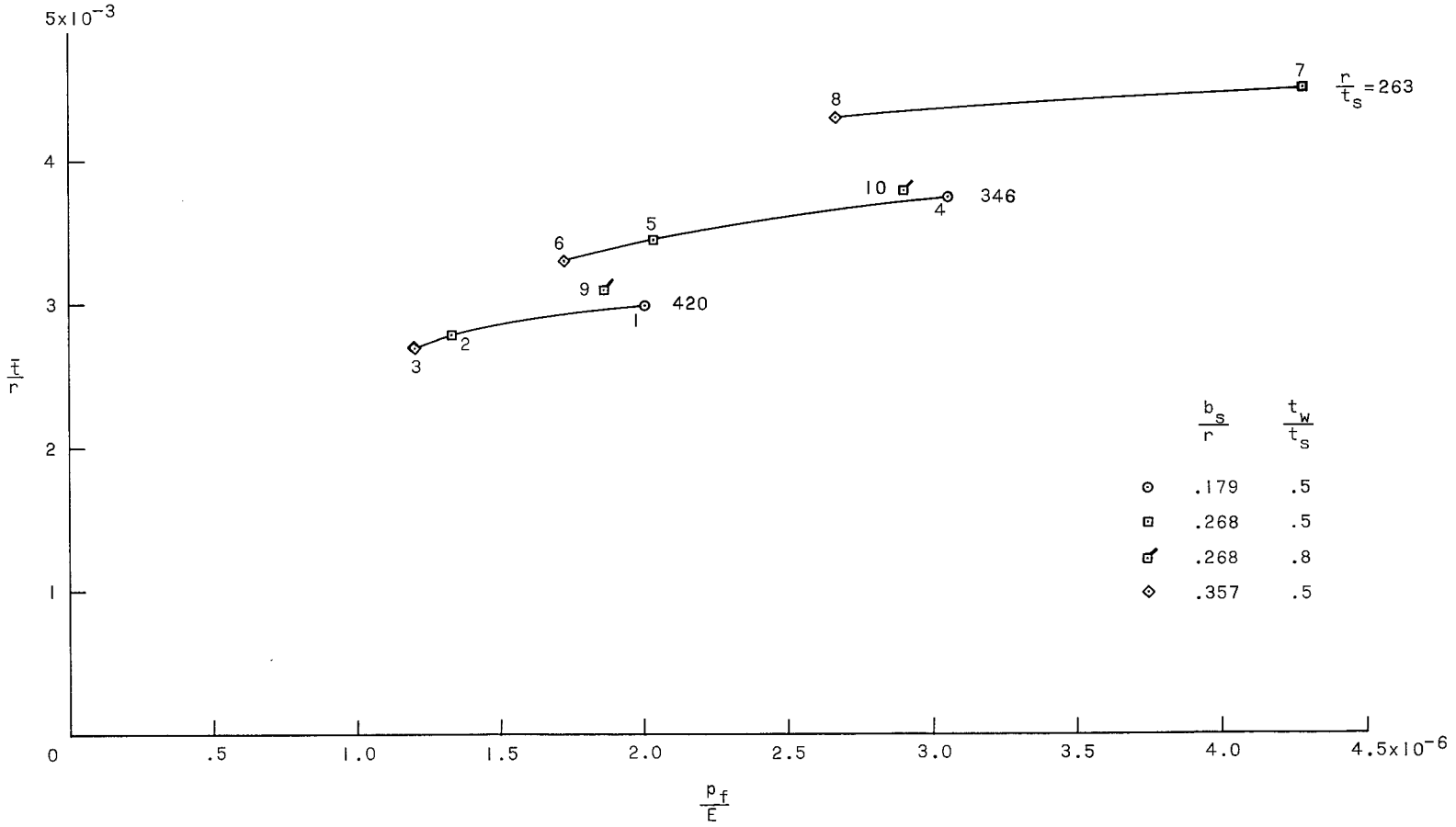


Figure 8.- Structural efficiency plot of collapse pressures of cylinders. L/r = 1.214; L = 17.0 in. (43.2 cm); numbers beside test points are cylinder numbers.

*"The aeronautical and space activities of the United States shall be conducted so as to contribute . . . to the expansion of human knowledge of phenomena in the atmosphere and space. The Administration shall provide for the widest practicable and appropriate dissemination of information concerning its activities and the results thereof."*

—NATIONAL AERONAUTICS AND SPACE ACT OF 1958

# NASA SCIENTIFIC AND TECHNICAL PUBLICATIONS

TECHNICAL REPORTS: Scientific and technical information considered important, complete, and a lasting contribution to existing knowledge.

TECHNICAL NOTES: Information less broad in scope but nevertheless of importance as a contribution to existing knowledge.

TECHNICAL MEMORANDUMS: Information receiving limited distribution because of preliminary data, security classification, or other reasons.

CONTRACTOR REPORTS: Technical information generated in connection with a NASA contract or grant and released under NASA auspices.

TECHNICAL TRANSLATIONS: Information published in a foreign language considered to merit NASA distribution in English.

TECHNICAL REPRINTS: Information derived from NASA activities and initially published in the form of journal articles.

SPECIAL PUBLICATIONS: Information derived from or of value to NASA activities but not necessarily reporting the results of individual NASA-programmed scientific efforts. Publications include conference proceedings, monographs, data compilations, handbooks, sourcebooks, and special bibliographies.

***Details on the availability of these publications may be obtained from:***

SCIENTIFIC AND TECHNICAL INFORMATION DIVISION

NATIONAL AERONAUTICS AND SPACE ADMINISTRATION

**Washington, D.C. 20546**